Astron. Astrophys. 214, 168–178 (1989)

ASTRONOMY
AND
ASTROPHYSICS

Carbon abundance in the primaries of six Algol-type stars*

H. Cugier

Wrocław Astronomical Observatory, Kopernika 11, PL-51-622 Wrocław, Poland

Received June 27, accepted October 5, 1988

Summary. We performed the abundance analysis of carbon in six Algol-type stars using IUE archival data. In order to interpret the observed spectra, both LTE and non-LTE line profiles are computed. We obtain a cosmic abundance of carbon, $\log N(\mathrm{C/H}) = -3.48$, in the primary components of δ Librae, U Sagittae, RS Vulpeculae and u Herculis. All these systems have mass ratios $q \geq 0.32$. In TX Ursae Majoris ($q = 0.31$) we obtain $\log\ N(\mathrm{C/H}) = -3.73 \pm 0.20$, whereas in U Coronae Borealis ($q = 0.29$) we find the same underabundance of carbon as in λ Tauri ($q = 0.26$) and β Persei ($q = 0.22$) investigated in Paper II, viz., $\log\ N(\mathrm{C/H}) = -3.89 \pm 0.20$.

The result is discussed in terms of the evolutionary status of Algol-type stars. In particular, the lack of substantial depletion of carbon (of the order of 2 dex.) is interpreted as caused by a large-scale mixing of matter in the investigated stars.

Key words: stars: binaries: close – stars: LTE and non-LTE abundances – UV radiation

1. Introduction

Large-scale transfer of mass from one component to the other is the most basic phenomenon in the evolution of close binary systems (e.g. Plavec, 1968; Paczynski, 1971 and De Greve, 1986). When a sufficiently large fraction of mass is lost by the originally more massive star, substantial changes in the surface relative abundances of H, He, C, N and O because of the CNO cycle are expected. β Lyrae, recently investigated by Balachandran et al. (1986), is an example of such a system. A carbon (^{12}C) deficiency and nitrogen (^{14}N) enrichment may be observed in classical Algol-type stars even if the mass loss does not expose very deep layers with H, He and O anomalies. This is caused by the fact that the CN part of the CNO cycle in massive stars takes place above the convective core (e.g. Iben, 1967).

Recently, Parthasarathy et al. (1983) reported an analysis of CN and CH molecular bands of the secondary (mass-losing) components in U Cep and U Sge. They found an underabundance of carbon $\Delta\log N(\mathrm{C/Fe}) = \simeq -0.5$ and an overabundance of nitrogen $\Delta\log(\mathrm{N/Fe}) \simeq 0.5$. The primary (mass-gaining) components of β Per and λ Tau were investigated by Cugier and Hardorp (1988b), hereinafter referred to as Paper II. They obtained $\Delta\log N(\mathrm{C/H}) \simeq -0.40$ in both cases. A ^{12}C-deficiency favours the generally accepted evolutionary status of Algol-type stars, but the observed carbon abundances in β Per and λ Tau are markedly larger than the expected ones. Cugier and Hardorp (1988b) suggested that a large-scale mixing of matter occurs in the investigated stars.

In the present paper we extend the carbon abundance analysis to the primary components of six additional Algol-type systems. We make use of the C II lines located in the UV region. The observations, taken from the International Ultraviolet Explorer (IUE) archival data released for general use, are discussed in Sect. 2. Basic data for the investigated stars are collected in Sect. 3. In particular, this section contains a determination of the effective temperature of the primary components from the observed UV flux distributions. In Sect. 4 a short discussion of circumstellar features of the C II resonance lines is given. Then the IUE observations are interpreted by means of LTE and non-LTE line-profile calculations in Sect. 5, and discussed in terms of the evolutionary status of Algol-type stars in Sect. 6. Finally, the main conclusions are summarized in Sect. 7.

2. Observational data

The observational material consists of several high resolution IUE images, obtained from the U.S.A. National Space Science Data Center. The images, listed in Table 1, were made through the large entrance aperture by means of the short wavelength primary (SWP) and long wavelength redundant (LWR) cameras. The third and fourth columns give the starting time (UT) of the exposures and the date. The fifth column contains the corresponding orbital phase. The exposure time is shown in the sixth column. Finally, the last column of Table 1 references to the first author of the observing program taken from IUE program reference code.

Most of the images used in this paper are well exposed (cf. Table 2 where the exposure classification codes taken from IUE merged log are shown). In the case of SWP 20853 we have $C = 1.5\,X$, which means that this spectrum is slightly overexposed in some wavelength regions. The images were carefully reprocessed using the standard IUE Spectral Image Processing System (IUE SIPS) scheme. In further analysis we used only the spectral regions from $\lambda = 1260$ Å to 1870 Å (SWP images) and from $\lambda = 2020$ Å to 3050 Å (LWR images), because of uncertainties in the background removal and ripple correction between adjacent orders outside these wavelength regions. The IUE flux distributions can be compared with TD-1 satellite observations of δ Lib and u Her, collected in the Ultraviolet Bright Star Spectrophotometric Catalogue (Jamar et al., 1976). For this

* Based on observations by the International Ultraviolet Explorer collected at the U.S.A. National Space Science Data Center.

Table 1. Journal of the IUE observations

Star	Image no.	U.T.	Date			φ	Exp.	Observer
δ Lib	SWP 11038	15^h28^m	1981	Jan	12	0.74	10^m00^s	J. Rahe
	LWR 9699	15 40	1981	Jan	12	0.74	5 00	J. Rahe
U Sge	SWP 14702	16 27	1981	Aug	9	0.52	24 00	M.J. Plavec
	SWP 20199	21 23	1983	Jun	11	0.06	25 00	G.E. McCluskey
	LWR 11279	16 58	1981	Aug	9	0.53	15 00	M.J. Plavec
	LWR 16136	20 54	1983	Jun	11	0.05	24 00	G.E. McCluskey
TX UMa	SWP 9143	20 23	1980	May	27	0.60	38 00	G.E. McCluskey
	SWP 10238	08 36	1980	Sep	28	0.92	45 00	G.J. Peters
	SWP 10913	23 14	1980	Dec	28	0.83	34 00	G.E. McCluskey
	SWP 10994	21 36	1981	Jan	7	0.07	42 00	G.J. Peters
	SWP 11027	23 18	1981	Jan	11	0.40	32 00	G.J. Peters
	LWR 7872	13 42	1980	May	27	0.51	25 00	G.E. McCluskey
	LWR 8903	09 25	1980	Sep	28	0.94	30 00	G.J. Peters
	LWR 9596	22 28	1980	Dec	28	0.82	22 00	G.E. McCluskey
	LWR 9662	20 59	1981	Jan	7	0.07	30 00	G.J. Peters
U CrB	SWP 9980	12 25	1980	Sep	1	0.32	55 00	G.J. Peters
	SWP 9994	11 22	1980	Sep	3	0.88	45 00	G.J. Peters
	LWR 8692	13 50	1980	Sep	1	0.34	38 00	G.J. Peters
	LWR 8703	12 11	1980	Sep	3	0.90	32 00	G.J. Peters
RS Vul	SWP 20759	20 53	1983	Aug	23	0.14	45 00	P. Koubsky
	SWP 20796	20 44	1983	Aug	25	0.59	45 00	P. Koubsky
	LWR 16652	20 27	1983	Aug	23	0.14	22 00	P. Koubsky
	LWR 16668	20 15	1983	Aug	25	0.59	22 00	P. Koubsky
u Her	SWP 20596	14 47	1983	Aug	3	0.95	01 40	L.N. Hobbs
	SWP 20853	17 42	1983	Aug	30,	0.17	02 12	P.K. Barker
	LWR 16511	14 52	1983	Aug	3	0.95	01 20	L.N. Hobbs

purpose the IUE images were broadened to spectral resolution of the TD-1 observations and the flux ratios, $FR = F(\text{IUE})/F(TD\text{-}1)$ were calculated. We omitted the TD-1 observations at $\lambda = 2740$ Å, which are located below the IUE data by about 20% (cf. also Barylak, 1985). The mean values of FR are shown in the fifth column of Table 2 together with the standard errors. Unfortunately, there are no TD-1 observations of the other Algol-type stars investigated in the present paper. Therefore, we used the following procedure. The IUE spectra were convolved with a gaussian profile, $\sim \exp(-(V/V_G)^2)$ with the parameter V_G equal to 6 Å and 8 Å for SWP and LWR images, respectively. These data were used to construct the mean UV flux distribution of a given star by co-adding images with the weights proportional to the exposure continuum level above the local background, shown in the fourth column of Table 2. Next, we calculated the flux ratios, $FR = F(\text{image})/F(\text{mean})$, for the individual images at wavelength points spaced by 5 Å. The mean values of FR are given in the fifth column of Table 2. TX TMa, U CrB, RS Vul and u Her show almost the same relative flux distribution at different orbital phases. Only LWR images of U Sge differ somewhat more markedly from each other.

In the present paper we are mainly interested in an analysis of the UV 1 (1334.53 Å, 1335.66 Å and 1335.71 Å) and UV 11 (1323.86 Å, 1323.91 Å, 1323.95 Å and 1324.00 Å) multiplets of C II. The accuracy of the observed line profiles was estimated as described by Cugier and Hardorp (1988a, hereinafter Paper I), cf. also Paper II. The last two columns of Table 2 show rms noise amplitudes obtained for the orders 104 and 103 of the SWP images, where the C II lines are located.

3. Basic data for the primary components

The program stars include six Algol-type binaries, listed in Table 3, where details are given together with references for masses and radii. The application of spectrum synthesis requires the specification of the effective temperature T^1_{eff}, gravity $\log g^1$, microturbulence ξ and the projected rotational velocity $v \sin i$ for the primary components. In the case of U Sge, we adopted Dobias and Plavec's (1985) determination of T^1_{eff} and $\log g^1$. The effective temperatures of the primary stars of δ Lib, TX UMa, U CrB, RS Vul and u Her were derived from the observed UV flux distributions, discussed in Sect. 2, by comparison with theoretical fluxes from Kurucz's (1979) grid of models with a solar abundance of elements. In the theoretical fluxes we also included contributions of the secondary components. $\log g^2$ were calculated from the observed masses and radii, shown in Table 3, and T^2_{eff} were estimated from the spectral types, using the temperature scale of Popper (1980). Furthermore, the observed flux distributions were dereddened by means of the mean extinction curve given by Savage and Mathis (1979). We obtained the best fit of the theoretical fluxes to the observed ones, in the least-squares sense, by adjusting the parameters: T^1_{eff}, $\log g^1$ and $E(B-V)$.

The primary component of δ Lib is an AO V star, while the secondary is probably an early G type star, following Koch (1962), Sahade and Hermandez (1963), and Tomkin (1978). From the observed UV flux distribution we obtained: $T^1_{\text{eff}} = 9875$ K, $\log g^1 = 4.4$ and $E(B-V) = 0\overset{m}{.}01$, assuming $T^2_{\text{eff}} = 5800$ K for the secondary on the basis of its spectral type and adopting

Table 2. Estimated accuracy of the IUE images

Star	Image no.	Exposure code	Continuum level	FR	rms orders 104	rms orders 103
δ Lib	SWP 11038	501	> 150	1.018 ± 0.010	0.06	0.06
	LWR 9699	402	> 100	1.039 ± 0.010	0.06	0.06
U Sge	SWP 14702	C = 260, B = 110	150	1.054 ± 0.004	0.06	0.05
	SWP 20199	C = 185, B = 38	147	0.945 ± 0.004	0.06	0.05
	LWR 11279	C = 225, B = 50	175	1.147 ± 0.008		
	LWR 16136	C = 245, B = 40	205	0.874 ± 0.005		
TX UMa	SWP 9143	C = 240, B = 46	194	1.019 ± 0.004	0.05	0.05
	SWP 10238	C = 270, B = 57	213	0.997 ± 0.002	0.04	0.04
	SWP 10913	C = 230, B = 40	190	0.993 ± 0.002	0.04	0.06
	SWP 10994	C = 255, B = 48	207	0.992 ± 0.002	0.04	0.05
	SWP 11027	C = 215, B = 40	175	1.008 ± 0.003	0.06	0.08
	LWR 7872	C = 230, B = 40	190	1.020 ± 0.003		
	LWR 8903	C = 260, B = 43	217	0.996 ± 0.002		
	LWR 9596	C = 230, B = 35	195	1.018 ± 0.002		
	LWR 9662	C = 255, B = 40	215	0.970 ± 0.002		
U CrB	SWP 9980	C = 240, B = 60	180	1.006 ± 0.003	0.03	0.04
	SWP 9994	C = 170, B = 50	120	0.991 ± 0.004	0.06	0.09
	LWR 8692	C = 245, B = 50	195	1.006 ± 0.002		
	LWR 8703	C = 220, B = 42	178	0.993 ± 0.002		
RS Vul	SWP 20759	511	> 150	1.006 ± 0.002	0.07	0.08
	SWP 20796	511	> 150	0.994 ± 0.001	0.07	0.08
	LWR 16652	511	> 150	1.004 ± 0.002		
	LWR 16668	512	> 150	0.996 ± 0.001		
u Her	SWP 20596	C = 170, B = 33	147	0.742 ± 0.010	0.06	0.06
	SWP 20853	C = 1.5X,B = 43	—	1.050 ± 0.015	0.05	0.05
	LWR 16511	C = 180, B = 33	147	0.736 ± 0.008		

Table 3. The program stars

Star	HD	Sp	P [d]	$M_{1,2}$ [$M_\odot$]	$R_{1,2}$ [$R_\odot$]	Ref.
δ Lib	132742	B9.5 V	2.327	4.7 ± 0.2	4.12 ± 0.09	T78
		G		1.7 ± 0.2	3.86 ± 0.06	
U Sge	181182	B8 V	3.381	5.7 ± 0.3	4.2 ± 0.3	T79, DP85
		G4 III		1.9 ± 0.1	5.3 ± 0.2	
TX UMa	93033	B8 V	3.063	3.6 ± 1.1	2.3 ± 0.2	GM81
		gF2		1.1 ± 0.3	4.1 ± 0.4	
U CrB	136175	B6 V	3.452	4.8	3.3	BT81
		F8 III		1.4	4.5	
RS Vul	180939	B6 V	4.478	4.8	4.5	HH71
		F		1.4	5.4	
u Her	156633	B3 III	2.051	7.8 ± 0.4	5.0 ± 0.1	V85
		B7 III		2.82 ± 0.13	4.4 ± 0.2	

References for masses and radii:
BT81: Batten and Tomkin (1981)
DP85: Dobias and Plavec (1985)
GM81: Giuricin and Mardirossian (1981)
HH71: Hutchings and Hill (1971)
T78: Tomkin (1978)
T79: Tomkin (1979)
V85: van der Veen (1985)

geometrical elements of the system given by Tomkin (1978). From the TD-1 satellite observations mentioned in Sect. 2 we found: $T^1_{eff} = 9900$ K, $\log g^1 = 4.4$ and $E(B-V) = 0^m.00$. The effective temperature of about 9900 K corresponds well to the AO V spectral type of the primary component. δ Lib appears to be a virtually unreddened star, $E(B-V) = 0^m.01 \pm 0^m.01$, which is in agreement with the results of Olson (1975), Lacy (1979) and Eggen (1982). $\log g^1 = 4.4$ exceeds markedly the logarithmic surface gravity, 3.88, calculated from the observed mass and radius shown in Table 3 and also the value obtained by Olson (1975) from the hydrogen line profiles, $\log g^1 = 3.99$. Fortunately, an error in $\log g^1$ of the order of ± 0.5 dex. does not play a crucial role in our determination of T^1_{eff}. We estimated the accuracy of T^1_{eff} by varying T^2_{eff} $\log g^1$ and $E(B-V)$, i.e., $\Delta \log g^1 = \pm 0.50$, $\Delta E(B-V) = \pm 0^m.02$ and $\Delta T^2_{eff} = \pm 500$ K results in $\Delta T^1_{eff} = \pm 200$ K. In the subsequent analysis we adopted the following values: $T^1_{eff} = 9900 \pm 200$ K, $\log g^1 = 4.0 \pm 0.1$, $E(B-V) = 0^m.01 \pm 0^m.01$, $d = 114 \pm 10$ pc. and $T^2_{eff} = 5800 \pm 500$ K (cf. Table 4). We would like to note that the given above distance $d = 114 \pm 10$ pc. agrees very well with the distance modulus of $5^m.30$ ($d = 115$ pc.) derived by Eggen (1982).

In Batten's et al. (1978) catalogue of binary stars, TX UMa appears as a B8 V + gF2 system. This spectral classification of the primary is in agreement with the colour indices $(B-V)_0 = -0^m.09$ and $(U-B)_0 = -0^m.41$ given by Koch (1961) and using FitzGerald's (1970) intrinsic colours of stars as a function of MK class. Our final solution is shown in Table 4, and the quality of the fit can be judged from Fig. 1, which can be regarded as representative for stars investigated in this paper.

The observed UV flux distribution of U CrB leads to T^1_{eff} and $\log g^1$ shown in Table 4, which is consistent with the spectral type B6 given by Hill et al. (1975) and Batten and Tomkin (1981). The secondary has been classified GO III-IV (Plavec and Polidan, 1976) or F8 III-IV (Batten and Tomkin, 1981.)

The primary component of RS Vul is a B5-B4 type star, whereas the secondary is a gF9 or GO type star according to Plavec (1967), Hutchings and Hill (1971), Cester et al. (1977) and Popper (1980). RS Vul shows the largest reddening among stars investigated in this paper. In fact, the observed UV flux distribution shows an extinction bump at $\lambda = 2200$ Å (cf. lower part of Fig. 2), $E(b-y) = 0^m.18$ (Olson, 1975) and $E(V-R) = 0^m.229$ (Lacy, 1979). Using Hutchings and Hill's (1971) geometrical elements, we obtained the best least-squares fit of Kurucz's (1979)

Table 4. T^1_{eff}, $\log g^1$ of the primary components and $E(B-V)$

Star	T^1_{eff}	Log g^1	$E(B-V)$ [mag]
δ Lib	9900 ± 200	4.00 ± 0.10	0.01 ± 0.02
U Sge[a]	12250 ± 250	3.90 ± 0.10	0.06
TX UMa	12900 ± 300	4.00 ± 0.15	0.00 ± 0.02
U CrB	14800 ± 300	3.80 ± 0.20	0.02 ± 0.02
RS Vul	16700 ± 400	4.00 ± 0.30	0.27 ± 0.02
u Her	22200 ± 1500	4.00 ± 0.10	0.02 ± 0.02

[a] From Dobias and Plavec (1985)

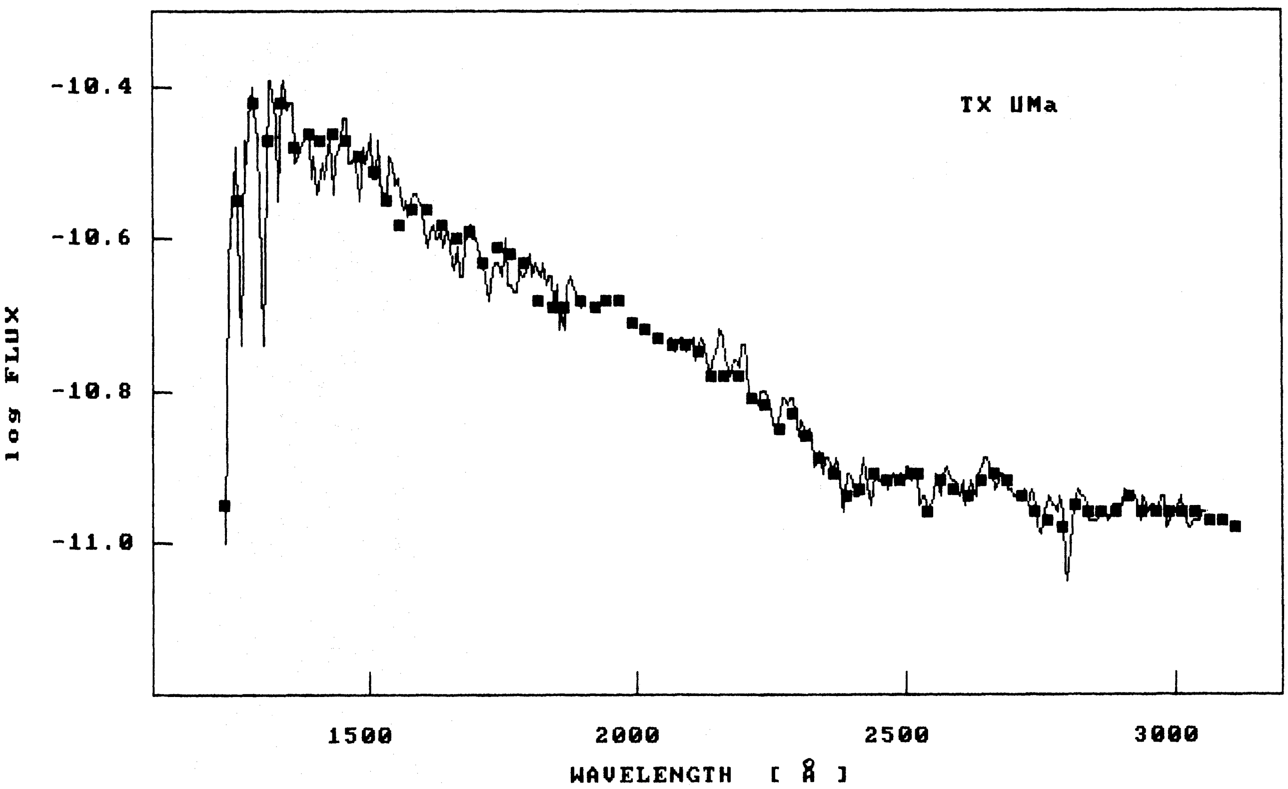

Fig. 1. The observed UV flux distribution of TX UMa is well matched by an interpolated Kurucz model atmosphere for $T^1_{eff} = 12900$ K and $\log g^1 = 4.0$ (primary component). A small contribution of the secondary component with $T^2_{eff} = 6700$ K and $\log g^2 = 3.25$ has been included in the theoretical flux distribution. The observed mean flux distribution is shown as a continuous line

models to the IUE flux distributions at $\varphi = 0.14$ and 0.51 for $T^1_{\rm eff}$, log g^1 and $E(B-V)$ shown in Table 4. This solution is also displayed in Fig. 2 (filled squares) in comparison with the dereddened UV flux distribution (upper part).

Finally, several analyses of the light curve of u Her were carried out in an attempt to determine physical parameters of the system (e.g. van der Veen (1985), Jabbar et al. (1987) and references cited therein). Assuming $T^2_{\rm eff} = 12000$, 13000 and 14000 K for the secondary star we obtained the best fits of the theoretical fluxes to the IUE observations for log $g^1 = 3.70$ and $E(B-V) = 0^m.02$ independently of $T^2_{\rm eff}$. The resulting effective temperature of the primary star is shown in Fig. 3 as a function of $T^2_{\rm eff}$. In this figure we also plotted van der Veen's (1985) solutions given by his Eqs. 3 and 4. As one can see, a consistent solution is obtained for $T^1_{\rm eff} = 22200$ K and $T^2_{\rm eff} = 13300$ K. These effective temperatures are the same, within the error limits, as those listed by Popper (1980).

4. Discussion of circumstellar features of the C II resonance lines

In several classical Algol-type stars UV spectra reveal circumstellar features at the Si IV 1400 Å, Al III 1860 Å, Mg II 2800 Å, etc. resonance multiplets. These features are phase- and time-dependent (e.g. Peters and Polidan, 1984 and Cugier and Molaro, 1984). In the cases of δ Lib, RS Vul and u Her analysed in the present paper, we found no clear evidence for circumstellar features either at Si IV, Al III, Mg II, C II resonance lines or at C II 1324 Å subordinates lines.

In U Sge, variable Si IV and C IV resonance lines were found by McCluskey and Kondo (1984). Dobias and Plavec (1985) reported that this system may be considered as nearly dormant, however emission lines of highly ionized species were detected in an IUE spectrum taken during a total primary eclipse. SWP images of U Sge analysed in this paper (cf. Table 1) were obtained at orbital phases $\varphi = 0.06$ and 0.52. The spectra are almost the same in the wavelength region from $\lambda = 1320$ Å to 1340 Å, including the C II line profiles at $\lambda = 1335$ Å and $\lambda = 1324$ Å. The good agreement between calculated line profiles and the observed ones indicates that the C II multiplets are indeed not influenced by circumstellar features.

TX UMa is an interacting Algol-type system for which variable Si IV resonance lines were detected by Peters and Polidan (1984). They report, however, that the Si IV lines are not always present and that the observations at the orbital phase $\varphi = 0.40$ (SWP 11027) represent a quiet period. We selected this spectrum for our analysis of the C II line profiles. A comparison with calculated line profiles shows that the observed C II lines are not influenced by circumstellar features, probably with the exception of the line cores of the resonance multiplet. The C II 1324 Å line profiles are practically the same in all IUE images of TX UMa listed in Table 1, whereas the C II 1335 Å lines reveal weak additional absorption components at $\varphi = 0.92$, 0.83 and 0.07. In other words, the C II resonance lines match the behaviour of the Si IV, Mg II and A1 III resonance lines, but in a much lesser degree.

U CrB is another example of a classical Algol-type system which shows variable Si IV lines (cf. Peters and Polidan, 1984).

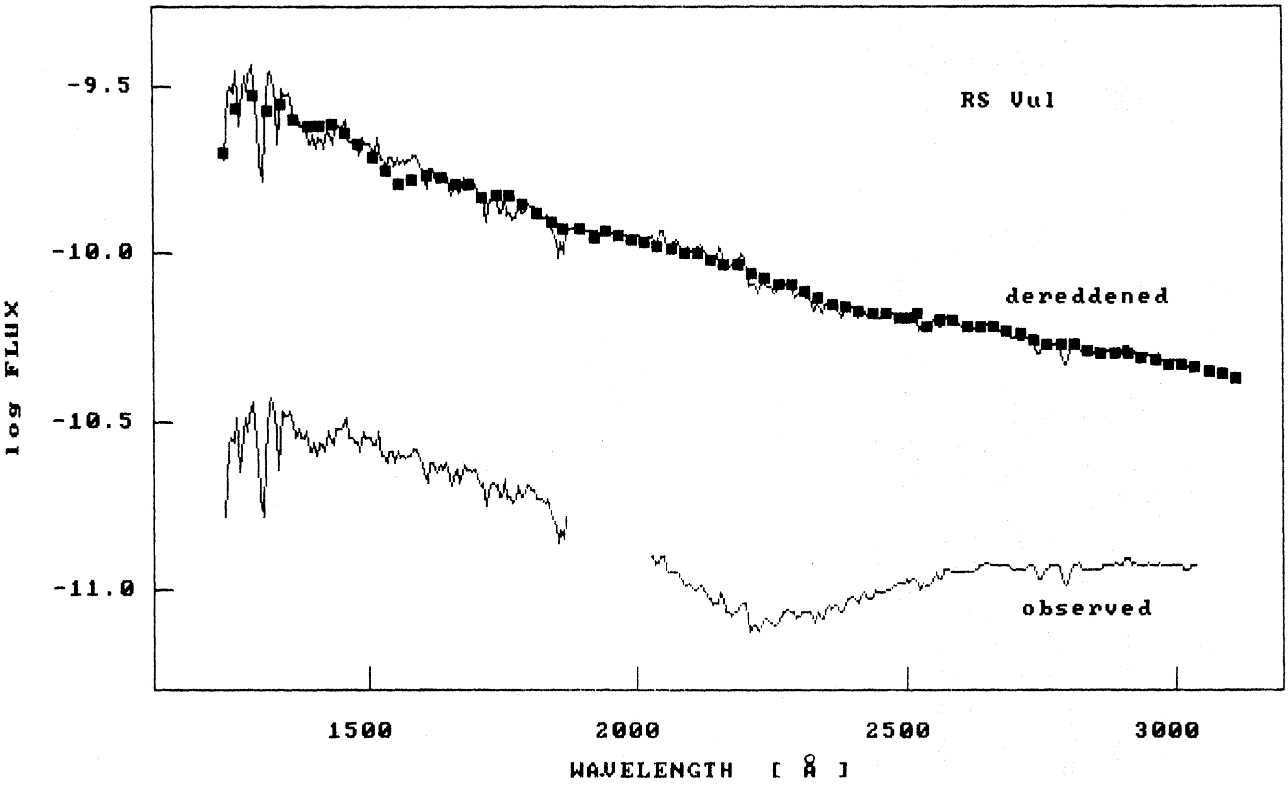

Fig. 2. The dereddened UV flux distribution of RS Vul (upper part) is well matched by interpolated Kurucz model atmospheres for $T^1_{\rm eff} = 16700$ K, log $g^1 = 4.0$ (primary component) and $T^2_{\rm eff} = 6000$ K, log $g^2 = 3.1$ (secondary component). The dereddened mean flux distribution is shown as a continuous line. The lower part shows the observed (reddened) flux distribution of RS Vul

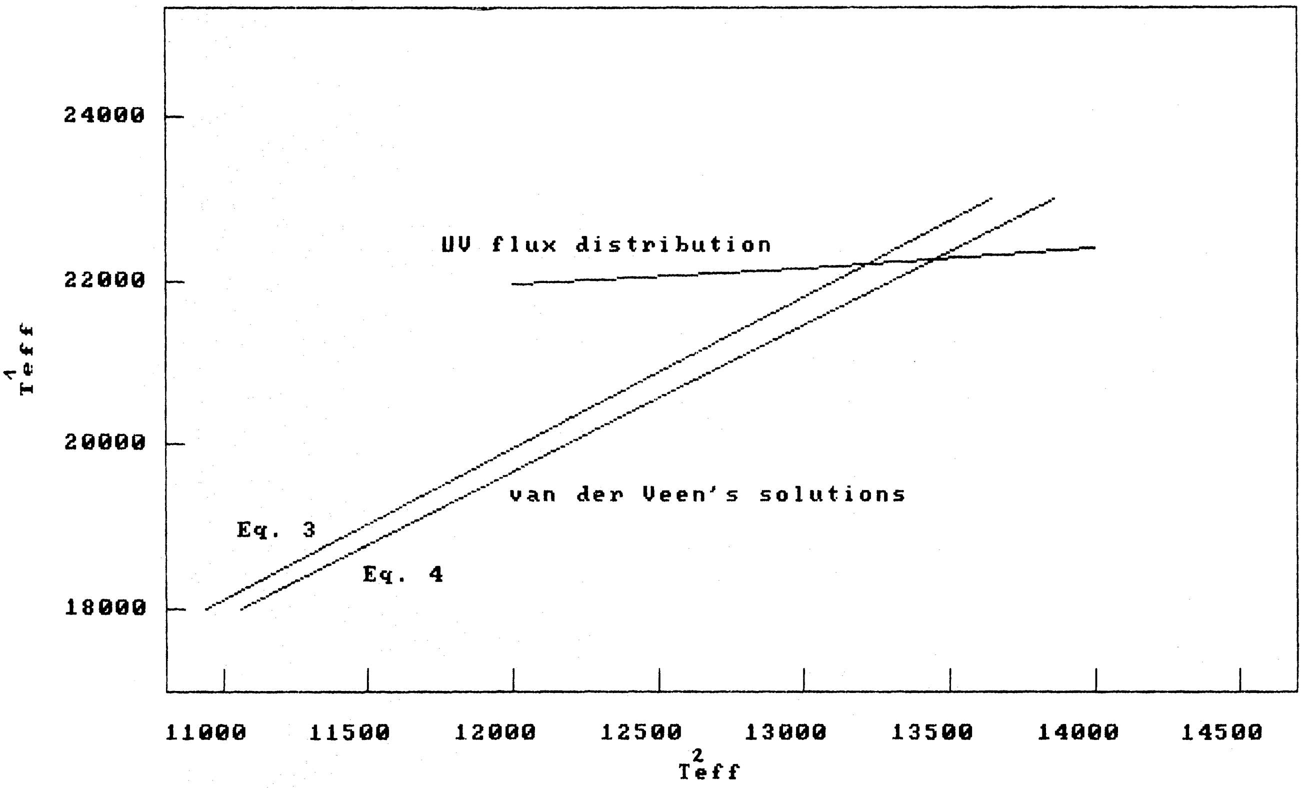

Fig. 3. The effective temperature of the primary component, $T^1_{\rm eff}$, as a function of $T^2_{\rm eff}$ for u Her. Both visual light curve analysis (taken from van der Veen's, 1983 Eqs. 3 and 4) and UV flux distribution give a consistent solution for $T^1_{\rm eff} = 22200$ K and $T^2_{\rm eff} = 13300$ K

Si IV was at its maximum strength at $\varphi = 0.88$, moderately strong at $\phi = 0.53$ and 0.62, but no Si IV was observed at $\varphi = 0.32$ (SWP 9980). According to Peters and Polidan, A1 III resonance lines vary in step with those of Si IV. We would like to add that also Mg II resonance lines at $\lambda = 2800$ Å match the behaviour of the Si IV and A1 III. Additional absorption components of the Mg II lines are clearly seen in the spectrum LWR 8703 ($\varphi = 0.90$), but not in LWR 8692 ($\varphi = 0.34$). Even at $\varphi = 0.88$, when the Si IV, Al III and Mg II lines have maximum strengths, the C II lines are not influenced markedly by circumstellar components. The C II 1324 Å lines are practically the same at all orbital phases mentioned above. In the further analysis we used SWP 9980 ($\varphi = 0.32$) image of U CrB.

5. Carbon abundance analysis

The observed UV flux of radiation comes mainly from the primary components (A0 to B2.5 main-sequence stars) of the investigated systems (cf. Sect. 3). This enables us to study photospherical lines of the primaries in the far UV region without taking into account the very small contributions from the secondaries (F to G type subgiants). The method of analysis is essentially the same as that described in Papers I and II. The sensitivity of the C II lines to model calculations is shown in Table 5, where some LTE and non-LTE calculations are presented in terms of the total equivalent widths, W_λ. The calculations were performed using the model atmospheres of Kurucz (1979), Borsenberger and Gros (1979) and Mihalas (1972), distinguished by letters K, B&G and M in the last column of the Table.

The C II line profiles are rather insensitive to $T_{\rm eff}$, log g and ξ for the Kurucz models in the range $10000 \leq T_{\rm eff} \leq 18000$ K. In hotter atmospheres, the C II lines depend much more strongly on $T_{\rm eff}$, as well as on the grid of model atmospheres, used in the analysis. The latter reflects differences in atmospheric structure caused by the line-blanketing effect. As it is well known, the Kurucz (1979) grid consists of fully line-blanketed models, whereas Mihalas (1972) models are only hydrogen line-blanketed. We would like to add here that our calculations of the C II lines at $\lambda = 4262$ Å and $\lambda = 3920$ Å, using Kurucz's (1979) model atmospheres and the cosmic abundance of carbon agree fairly well with observations of single stars reported by Kane et al. (1980). Such an agreement is not obtained when only hydrogen line-blanketed models are used (Kane et al., 1980 and Lennon, 1983). A more detailed discussion of the C II 4262 Å and 3920 Å lines will be given in a future paper.

In Table 5, the non-LTE calculations performed under the assumption of the complete redistribution are indicated by non-LTE/CR. The partial redistribution calculations are shown as non-LTE/PR. The reader is referred to Paper I, where a detailed discussion of the C II resonance lines is given for models in the range $9500 \leq T_{\rm eff} \leq 17500$ K. In the present paper we extend these calculations to a non-LTE model atmosphere with $T_{\rm eff} = 22500$ K and log $g = 4.0$ (taken from Mihalas, 1972) in order to interpret the C II lines of u Her. In addition to C II and C III levels listed in Table 4 of Paper I, we took into account the 3s ^2S, 3d ^2D, 4s ^2S, 4p^2 P^0 and 4 f$^2F^0$ levels of C II, and $2p^2$ ^3P, 3s ^3S, 3p $^3P^0$ and 3d ^3D levels of C III. Atomic data used in Paper I were supplemented from Nussbaumer and Storey (1981), Wiese et al. (1966) and Hofsaess (1979).

Table 5. The total equivalent widths of the C II lines at $\lambda = 1335$ Å and $\lambda = 1324$ Å

T_{eff}	Log g	ξ [km s^{-1}]	Log N(C/H)	W_λ^a 1335 Å	W_λ^b 1324 Å	Comment
10000	4.0	2	−3.430	3.205	0.216	LTE, K
10000	4.0	2	−3.129	4.086	0.237	LTE, K
10000	4.0	2	−3.731	2.464	0.199	LTE, K
10000	4.0	2	−3.430	3.360		non-LTE/CR, B&G
10000	4.0	2	−3.430	3.602		non-LTE/PR, B&G
10000	3.5	2	−3.430	3.602	0.230	LTE, K
10000	4.0	5	−3.430	3.192	0.238	LTE, K
10500	4.0	2	−3.430	3.170	0.225	LTE, K
15000	4.0	2	−3.430	3.174	0.286	LTE, K
15000	4.0	2	−3.430	3.190	0.272	LTE, K
18000	4.0	2	−3.430	2.774	0.289	LTE, K
20000	4.0	2	−3.430	2.358	0.281	LTE, K
22500	4.0	2	−3.430	1.593	0.264	LTE, K
22500	4.0	2	−3.129	2.176	0.291	LTE, K
22500	4.0	2	−3.731	1.133	0.246	LTE, K
22500	4.0	2	−3.430	2.149	0.276	LTE, M
22500	4.0	2	−3.430	1.945		non-LTE/CR, M
22500	4.0	2	−3.430	1.623		non-LTE/PR, M
22500	3.5	2	−3.430	1.404	0.257	LTE, K
22500	4.0	2	−3.430	1.539	0.289	LTE, K

[a] Calculated from $\lambda = 1330.0$ Å to 1340.0 Å
[b] Calculated from $\lambda = 1322.5$ Å to 1326.0 Å

Table 6. The derived carbon abundances, ξ and $V \sin i$

Star	Log N(C/H) LTE	Non-LTE/CR	Non-LTE/PR	ξ [km s^{-1}]	$V \sin i$ [km s^{-1}]
δ Lib	-3.58 ± 0.15	-3.64 ± 0.20	-3.55 ± 0.20	2	75
U Sge	-3.50 ± 0.15	-3.54 ± 0.20	-3.43 ± 0.20	3	80
TX UMa	-3.80 ± 0.15	-3.85 ± 0.20	-3.73 ± 0.20	2	64
U CrB	-3.95 ± 0.15	-4.00 ± 0.20	-3.89 ± 0.20	2	48
RS Vul	-3.48 ± 0.15	-3.55 ± 0.20	-3.42 ± 0.20	2	90
u Her	-3.58 ± 0.30	-3.76 ± 0.30	-3.60 ± 0.30	2	120

Finally, in both LTE and non-LTE/PR calculations of the emergent C II resonance line profiles we also included blend contributions of other elements in the background opacity sources. The blends were treated under the LTE assumption with all details, exactly in the same way as in Paper I.

The derived carbon abundances are listed in Table 6, together with $V \sin i$ and ξ obtained in the best fit procedure. Figure 4 shows an example of the calculated spectra in comparison with the IUE observations of TX UMa. The lack of a complete list of spectral lines at the analysed wavelength region is the major source of discrepancies between the synthetic and observed spectra (cf. also Papers I and II). As mentioned above, the lack of a fully line-blanketed non-LTE model with $T_{eff} = 22200$ K causes some uncertainties in the analysis of u Her. From Table 5 one can see that LTE and non-LTE/PR calculations using Mihalas (1972) models differ between each other by $\Delta W_\lambda / W_\lambda = -24\%$, which corresponds to $\Delta \log N(C/H) = -0.20$. Assuming that LTE calculations performed for an LTE fully line-blanketed model should be corrected by -0.20 dex in order to estimate non-LTE effects, we have $\log N(C/H) = -3.38 \pm 0.30$. We conclude, therefore, that u Her shows an essentially cosmic abundance of carbon.

6. Discussion of some evolutionary aspects

As mentioned in Sect. 1, spectroscopic investigations of Algol-type stars offer a possibility to study stellar atmospheres with the chemical composition of matter, previously processed by the CNO nucleosynthesis in stellar interiors. Let us first examine the behaviour of the observed ^{12}C-abundance, given in the fourth column of Table 6, as a function of the mass ratio $q = M_l / M_g$. M_l corresponds to a mass-losing (cooler) component, whereas M_g

indicates a mass-gaining (hotter) star (cf. Table 3). Carbon abundances of β Per and λ Tau obtained in Paper II are also included here. As one can see from Fig. 5, all mass-accreting stars of the analysed systems with $q \geq 0.32$ have a cosmic abundance of carbon, whereas all systems with $q \leq 0.31$ show ^{12}C-depletion of about -0.4 dex. This indicates that β Per, λ Tau, TX UMa and U CrB are more advanced evolutionary, in the sense that they expose deeper layers of the originally more massive components, than those of δ Lib, U Sge, RS Vul and u Her.

According to Iben (1965) (cf. also Cugier and De Greve, 1988), the stellar region within which ^{12}C is being reduced to an equilibrium value with respect to ^{14}N expands outwards with time to greater mass fractions. However, ^{12}C-distribution becomes essentially fixed at the moment when the central hydrogen content, X_c, has decreased by about 15%. The case when the mass transfer between the components starts very close to ZAMS is probably not attractive for classical Algol-type systems (cf. Plavec et al., 1969). The very rapid "freezing" of the ^{12}C-profile at almost constant mass fractions, found for all models of 2.25 to 15 $M_\odot$ stars allows us to estimate ^{12}C-abundance in Algol-type stars provided that no mixing of matter has taken place during the evolution. A mass fraction, M_r, of the layers which are exposed now on the surface by the losers can be calculated from the following formula, obtained under the assumption of no mass loss from the system: $M_r = q(q^0+1)/(q^0(q+1))$, where q^0 is the initial mass ratio ($q^0 > 1.0$). The observed carbon depletion, $\Delta \log N(\mathrm{C/H}) = \log N(\mathrm{C/H}) + 3.48$, as a function of M_r calculated for $q^0 = 1$ is displayed in Fig. 6 by means of filled squares. The horizontal lines in this figure illustrate the amount of the change of M_r when $q^0 \to \infty$. In Fig. 6 we also plotted carbon abundance distributions vs. mass fraction taken from Iben (1965, 1966) for 3 and 5 $M_\odot$ stars. As mentioned in Paper II, the secondary in β Per is now exposed down to layers with $M_r < 0.36$, so that we can expect depletion of carbon of the order of 1.5 to 2.0 dex., much more than the observed 0.40 ± 0.20 dex. in the photosphere of the gainer. Furthermore, the fact that all systems with $0.22 \leq q \leq 0.31$ show the same carbon depletion in the gainers (cf. Fig. 5) can be, in our opinion, regarded as a conclusive evidence that a large-scale mixing of matter occurs in Algols.

The convective mixing cannot change markedly the original ^{12}C-distribution in a mass-losing component, unless the star's T_{eff} dropped to a very low value during the evolution. Published models of close binary evolution (cf. e.g., Ziółkowski, 1970, and van der Linden, 1987) indicate that T_{eff} of the losers decreases with time during the Algol-type phase of evolution. The maximum mass fraction contained in the outer convective zone can therefore be estimated from the actually observed values of T_{eff}. From the data discussed in Sect. 3 it follows that the effective temperatures of the losers are too high for a very deep outer convective zone, cf. also Paper II. Furthermore, the observed carbon depletion of the gainers does not depend on T_{eff} of the losers. This suggests that another kind of mixing may take place in Algols.

Cugier and De Greve (1988) have recently discussed the thermohaline diffusion, considered by Kippenhahn et al. (1980), as a mechanism responsible for mixing the carbon depleted, transferred material with the intrinsically normal material of the mass-accreting star. This process can take place if an inversion of

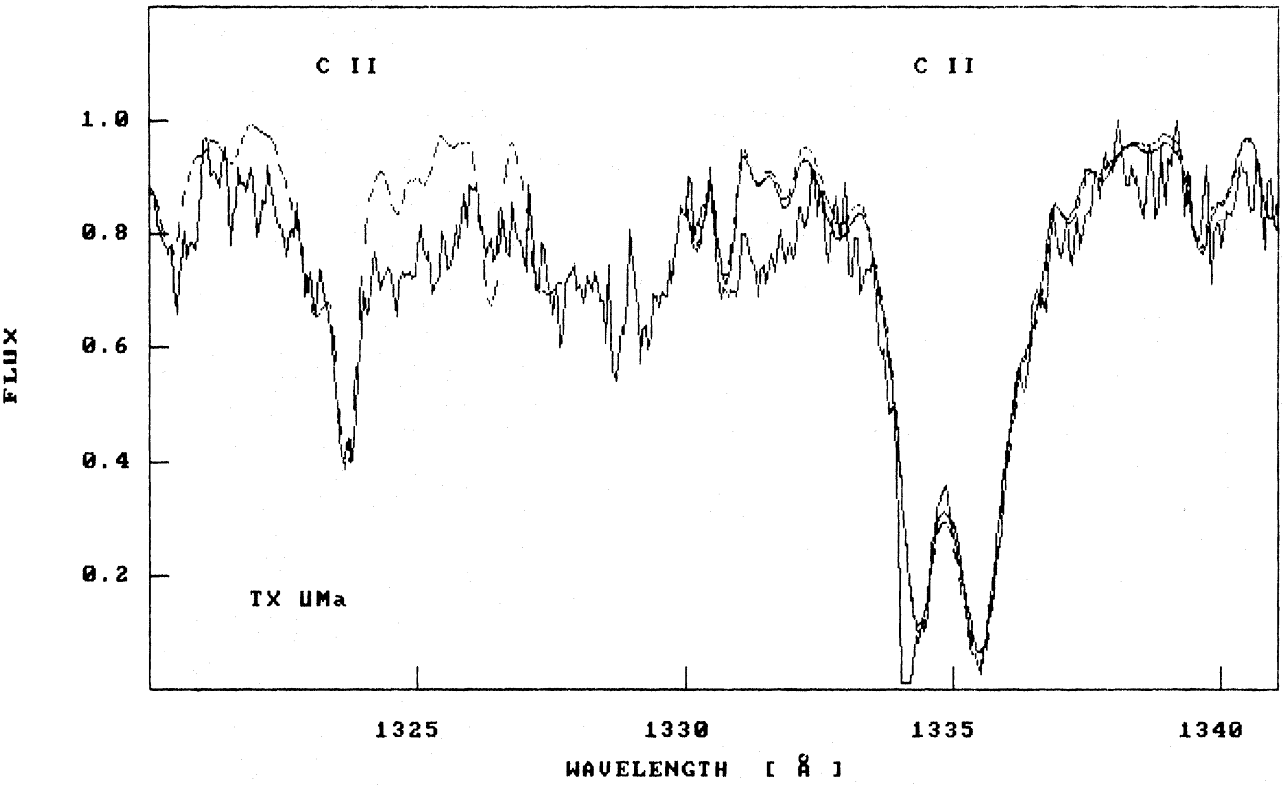

Fig. 4. High dispersion IUE observations of TX UMa are matched here by synthetic spectra. LTE calculations are shown as broken lines, while non-LTE/PR calculations, as a solid line

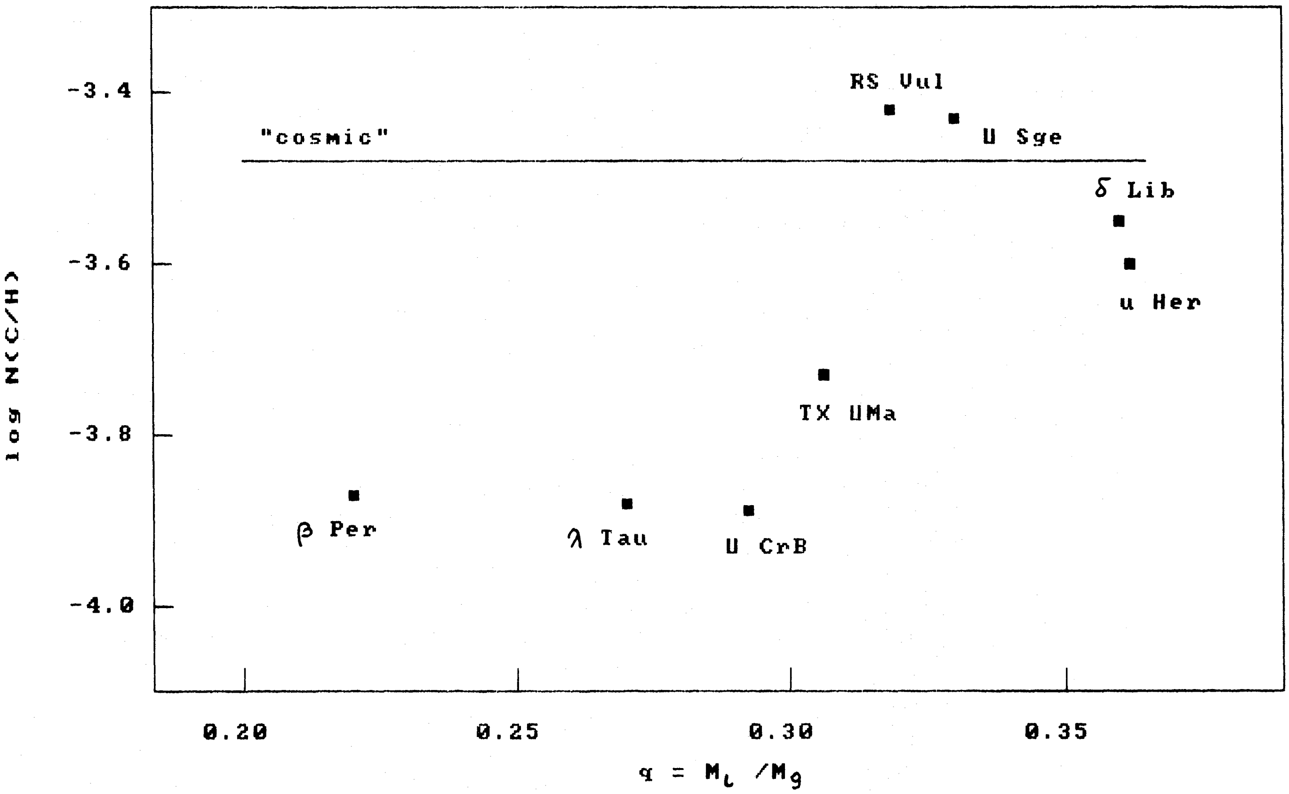

Fig. 5. The ^{12}C-abundance of the primary components as a function of the observed mass ratio, q

the mean molecular weight develops in the gainer due to accretion of helium-rich matter. On the other hand, there are good reasons to believe that mass exchange between components leads to fast rotation of the mass-accreting star. In this case mixing may be due to meridional circulations (cf. Tassoul and Tassoul, 1984).

The above considerations lead us to the conclusion that observations of both components can shed some light on the question in which component mixing takes place in Algols. There is some observational evidence that mixing may occur in the gainers. As mentioned in Sect. 1, Parthasarathy et al. (1983) found underabundance of carbon, -0.45 dex. and -0.50 dex., for the losers in U Cep and U Sge. Our analysis (cf. Sect. 5.2) indicates an essentially normal (cosmic) abundance of carbon in the gainer of U Sge. An estimated uncertainty of both determinations of the ^{12}C-abundance amounts to about ± 0.2 dex. Further observations are still necessary in order to establish whether differences in ^{12}C-abundance are really present in both components of Algol-type stars.

7. Conclusions

In the present study we had investigated six Algol-type stars, δ Lib, U Sge, TX UMa, U CrB, RS Vul and u Her, making use of IUE images obtained in the high resolution mode. The main result, the carbon abundance of the primary (mass-accreting) components, is shown in Table 6. When searching for correlations of the ^{12}C deficiency with system parameters, we succeeded in finding only one, namely with q. This might be taken to indicate that the systems with lower q are more advanced in evolution. However, since the early evolutionary calculations it is known that the fraction of mass lost by the loser is a complex function of the initial parameters. Furthermore, a comparison of the observed carbon abundances with the expected ones suggests that large-scale mixing of matter takes place in Algols. There is some evidence that mixing occurs in the gainers (cf. Sect. 6), but this suggestion should be verified by future abundance observations of both components.

On the other hand, there appears to be so little circumstellar material present in the investigated systems that they may be considered as dormant. Weak circumstellar features of UV resonance multiplets are phase- and time-dependent, cf. Sect. 4. Even when these features have maximum strengths, the observed flux distributions are matched very well by Kurucz's (1979) model atmospheres. This offers an opportunity to derive the properties of the primary components with great reliability.

Acknowledgements. The author would like to acknowledge partial support from the International Exchange Program SUNY during his stay at Stony Brook (U.S.A.) in 1984/5 where IUE observations were collected. The U.S. National Space Science Data Center provided the IUE tapes, and Richard Wagener explained the IUE programs at Stony Brook. The author also

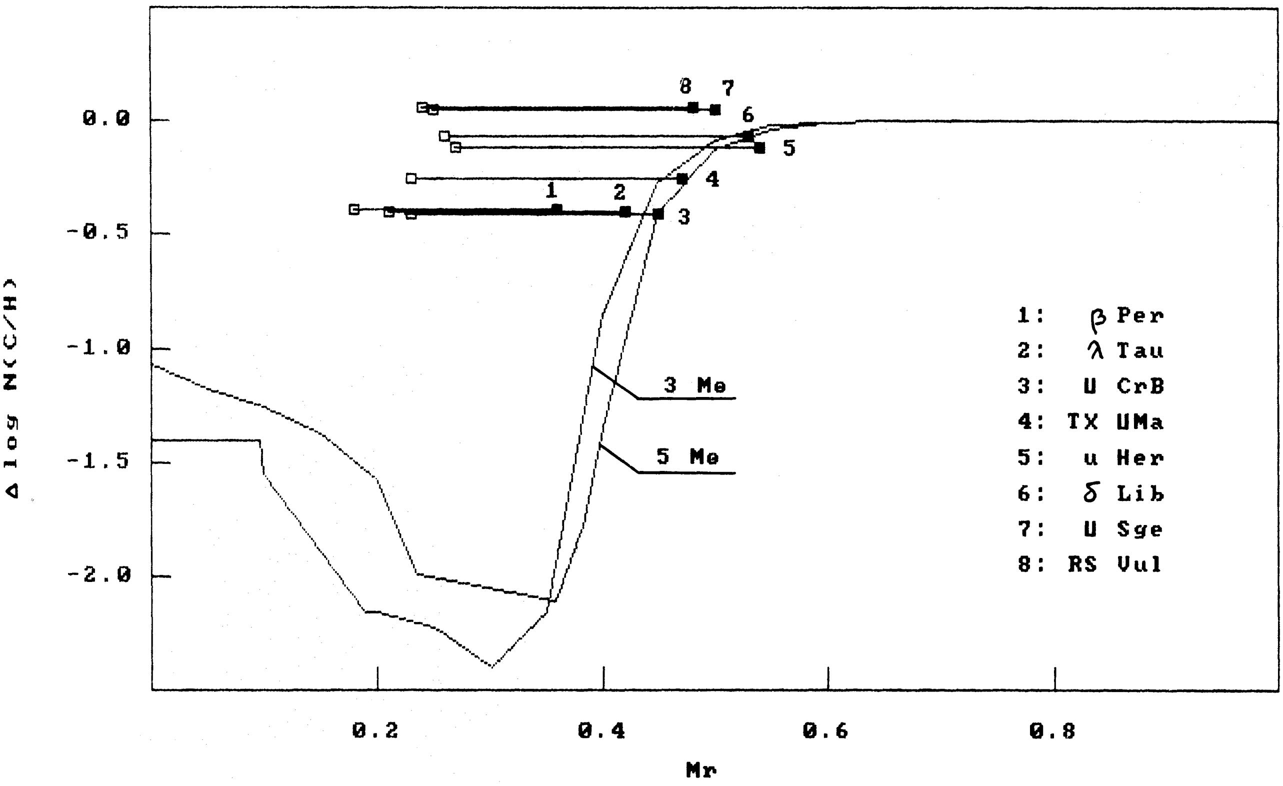

Fig. 6. The ^{12}C-depletion as a function of mass fraction, M_r, for 3 and 5 $M_\odot$ stars adopted from Iben (1965, 1966). The horizontal lines show the possible ranges of layers exposed now by the losers. Ordinates of these lines correspond to the observed ^{12}C-depletion of the primary components

wishes to acknowledge helpful discussions with Drs. J.P. De Greve, J. Hardorp and D.M. Peterson.

References

Balachandran, S., Lambert, D.L., Tomkin, J., Parthasarathy, M.: 1986, *Monthly Notices Roy. Astron Soc.* **219**, 479

Barylak, M.: 1985, *IUE ESA Newsletter* **22**, 25

Batten, A.H., Fletcher, J.M., Mann, P.J.: 1978, *Publ. Dominion Astrophys. Obs.* Vol. XV, No. 15

Batten, A.H., Tomkin, J.: 1981, *Publ. Dominion Astrophys. Obs.*, Vol. XV, No. 13

Borsenberger, J., Gros, M.: 1979, *Astron. Astrophys. Suppl.* **31**, 291

Cester, B., Fedel, B., Giuricin, G., Mardirossian, F., Pucillo, M.: 1977, *Astron. Astrophys.* **61**, 469

Cugier, H., De Greve, J.P.: 1988, in *Atmospheric Diagnostics of Stellar Evolution: Chemical Peculiarity, Mass Loss, and Explosion*, ed. K. Nomoto, Springer, Berlin Heidelberg, New York, p. 221

Cugier, H., Hardorp, J.: 1988a, *Astron. Astrophys.*, **197**, 163, (Paper I)

Cugier, H., Hardorp, J.: 1988b, *Astron. Astrophys.* **202**, 101 (Paper II)

Cugier, H., Molaro, P.: 1984, *Astron. Astrophys.* **140**, 105

De Greve, J.P.: 1986, *Space Sci. Rev.* **43**, 139

Dobias, J., Plavec, M.J.: 1985, *Publ. Astron. Soc. Pacific* **97**, 138

Eggen, O.J.: 1982, *Astrophys. J. Suppl.* **50**, 221

FitzGerald, M.P.: 1970, *Astron. Astrophys.* **4**, 234

Giuricin, G., Mardirossian, F.: 1981, *Astrophys. J. Suppl.* **46**, 1

Hill, G., Hildritch, R.W., Younger, F., Fisher, W.A.: 1975, *Mem. R. Astron. Soc.* **79**, 131

Hofsaess, D.: 1979, *Atomic Data and Nuclear Data Tables* **24**, 285

Hutchings, J.B., Hill, G.: 1971, *Astrophys. J.* **167**, 137

Iben, I.: 1965, *Astrophys. J.* **142**, 1447

Iben, I.: 1966, *Astrophys. J.* **143**, 483

Iben, I.: 1967, *Ann. Rev. Astron. Astrophys.* **5**, 571

Jabbar, S.R., Jabir, N.L., Fleyeh, H.A.: 1987, *Astrophys. Space Sci.* **135**, 377

Jamar, C., Macau-Hercot, D., Monfils, A., Thompson, G.I., Houziaux, L., Wilson, R.: 1976, *Ultraviolet Bright-Star Spectrophotometric Catalogue*, ESA SR-27

Kane, L., McKeith, C.D., Dufton, P.L.: 1980, *Astron. Astrophys.* **84**, 115

Kippenhahn, R., Ruschenplatt, G., Thomas, H.-C.: 1980, *Astron. Astrophys.* **91**, 175

Koch, R.H.: 1961, *Astron. J.* **66**, 230

Koch, R.H.: 1962, *Astron. J.* **67**, 130

Kurucz, R.L.: 1979, *Astrophys. J. Suppl.* **40**, 1

Lacy, C.H.: 1979, *Astrophys. J.* **228**, 817

Lennon, D.J.: 1983, *Monthly Notices Roy. Astron. Soc.* **205**, 829

Mc Cluskey, G.E., Kondo, Y.: 1984, in *Future of UV Astronomy based on Six Years of IUE Research*, NASA Conf. Publ. 2349, p. 382

Mihalas, D.: 1972, *NCAR Tech. Note*, Boulder, NCAR-TN/STR-76

Nussbaumer, H., Storey, P.J.: 1981, *Astron. Astrophys.* **96**, 91

Olson, E.C.: 1975, *Astrophys. J. Suppl.* **29**, 43

Paczyński, B.: 1971, *Ann. Rev. Astron. Astrophys.* **9**, 183
Parthasarathy, M., Lambert, D.L., Tomkin, J.: 1983, Monthly Notices Roy. Astron. Soc. **203**, 1063
Peters, G.J., Polidan, R.S.: 1984, *Astrophys. J.* **283**, 745
Plavec, M.J.: 1967, *Bull. Astron. Inst. Csl.* **18**, 334
Plavec, M.J.: 1968, *Adv. Astron. Astrophys.* **6**, 201
Plavec, M.J., Kriz, S., Horn, J.: 1969, *Bull. Astron. Inst. Csl.* **20**, 41
Plavec, M.J., Polidan, R.S.: 1976, in *Structure and Evolution of Close Binary Systems*, eds. P. Eggleton, S. Mitton, J.A.J. Whelan, Reidel, Dordrecht, p. 289
Popper, D.M.: 1980, *Ann. Rev. Astron. Astrophys.* **18**, 115
Sahade, J., Hermandez, C.A.: 1963, *Astrophys. J.* **137**, 945
Savage, B.D., Mathis, J.S.: 1979, *Ann. Rev. Astron. Astrophys.* **17**, 73
Tassoul, M., Tassoul, J.-L.: 1984, *Astrophys. J.* **279**, 384
Tomkin, J.: 1978, *Astrophys. J.* **221**, 608
Tomkin, J.: 1979, *Astrophys. J.* **231**, 495
van der Linden, T.J. : 1987, *Astron. Astrophys.* **178**, 170
van der Veen, W.E.C.J.: 1985, *Astron. Astrophys.* **145**, 380
Wiese, W.L., Smith, M.W., Glennon, M.: 1966, *Atomic Transition Probabilities*, NSRDS-NBS **4**
Ziółkowski, J.: 1970, *Acta Astron.* **20**, 213